We are IntechOpen, the world's leading publisher of Open Access books Built by scientists, for scientists

4,800
Open access books available

122,000
International authors and editors

135M
Downloads

Our authors are among the

154
Countries delivered to

TOP 1%
most cited scientists

12.2%
Contributors from top 500 universities

CLARIVATE ANALYTICS BOOK CITATION INDEX INDEXED

WEB OF SCIENCE™

Selection of our books indexed in the Book Citation Index in Web of Science™ Core Collection (BKCI)

Interested in publishing with us?
Contact book.department@intechopen.com

Numbers displayed above are based on latest data collected.
For more information visit www.intechopen.com

23

A Numerical Study on Time-Dependent Melting and Deformation Processes of Phase Change Material (PCM) Induced by Localized Thermal Input

Yangkyun Kim[1], Akter Hossain[1], Sungcho Kim[2] and Yuji Nakamura[1]
[1]*Hokkaido University,*
[2]*Sunchon National University*
[1]*Japan*
[2]*Korea*

1. Introduction

Deep understanding of fire damage triggered by combustion of electric wires is one of important issue in terms of the fire safety of automated facilities, such as factories, power plant etc. Combustion process of electric wire is, nevertheless, quite complicated since it consists of multi-phase, multi-dimensional time-dependent heat and mass transfer with chemical reactions in each phase and several fundamental processes are equally important so that it is relatively hard to simplify the system. Unlikely the conventional solid combustion, the metal rod in the wire could play an important role to determine the combustion process of the wire (Bakhman et al., 1981a, 1981b). In this way, the thermal interaction between the metal rod and surrounded insulated matter (mainly polymeric materials) is a leading key process in understanding the fire character of the wire (Umemura et al., 2002). However, this is not only the matter of concern; we have much serious problem to face with. As pointed, the combustible of electric wire is mainly the polymeric material surrounded by the (conductive) metal rod and the polymer does "melt" during the fire event. The shape of liquefied polymer freely modifies and sometimes tremendously deforms, thus, the precise tracking of the liquid-gas interface is one of important task since the major chemical reaction at the interface should govern the overall gasification rate (Blasi, 1991; Ross, 1994), i.e., gas-phase combustion behavior. As summarized, in order to predict the precise process of electric wire, the following three processes need to be modeled properly: 1) three-phase induced by chemical reactions (e.g., degraded pyrolysis), 2) deformation of interface of liquid phase, 3) heat transfer between metal rod and surrounded polymer (either melted and solid). Our ultimate goal is to understand each contribution properly and develop simplified model of wire combustion.

To this date, the precise experimental observation of combustion behavior of electric wire has been performed by authors' group (Nakamura et al., 2008a, 2008b, 2009), as shown schematically in Fig. 1. It shows the magnified still image of spreading flame over the specially-designed "model" wire (polyethylene-coated on the several kind of metal wires.

For details, see above references). During the combustion event, the coated polymer first liquefies to form large molten ball, and then decomposes to produce fuel gas released into the atmosphere. As notified clearly, it includes complex phenomena associated with the formation of molten layer; e.g., deformation of outer shape, bubble formation and its internal motion in the molten polymer etc. In our previous studies, it has been found that the size of molten polymer gradually increased during the flame spread over the wire. As a result of the size growth, "falls-off" of molten layer is frequently observed. Our precise observation data would be useful to validate the simulation and modelling, which is our goal as stated.

To achieve our ultimate goal; such as establishment of complete model of wire combustion, since the target is quite complex to handle as shown, it is preferable to take step-by-step. In this paper, let us consider the most fundamental case that there is no species transport and reaction, then main part to be modelled is the following two folds; one is how to consider the size change of the molten phase, and the other is how to handle the complex melting process. To simulate this, the governing equation requires the treatments of the discontinuity at the melting front caused by a higher energy than the latent heat of fusion at their interface, which is well known as Stefan problem. This results in transport properties varying considerably between phases, and hugely different rates of energy, mass and momentum transport from one phase to another.

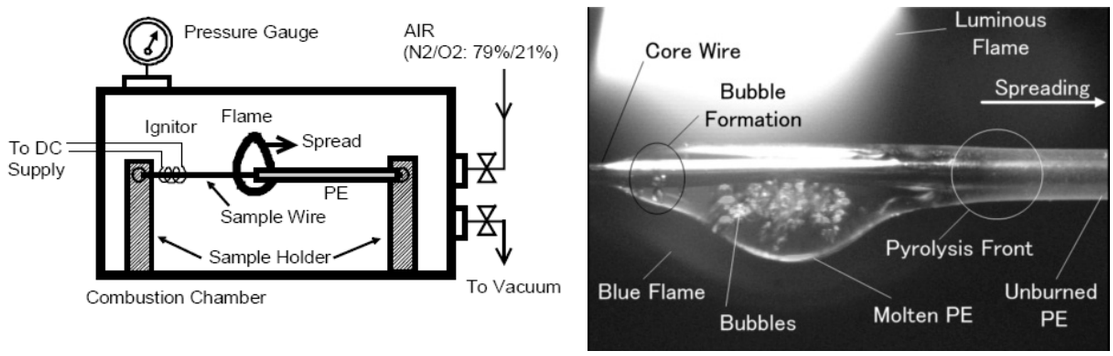

Fig. 1. Experimental set-up (left) and a typical observation of flame spreading (right) over polyethylene (PE) coated electric wire (Nakamura et al., 2009)

In the past, a few analytical methods offered an exact solution (Neumann, 1863). Even though they were mathematically robust, applicable ranges of solution are limited to one-dimensional cases of an infinite or semi-infinite region with simple initial and boundary conditions and constant thermal properties. Therefore treatments were extended to numerical analyses with finite difference and finite element methods. Particularly, because of their simplicity in formulation, finite difference methods are still used for a wide range of industrial processes. The essential feature of finite difference methods is that the latent heat absorption or release is accounted for in the governing energy equation by defining either a total enthalpy (Voller, 1986, 1987a; Gong, Z. X et al., 1997, 1999) or a specific heat capacity (Yang & He, 2010). Consequently, the numerical solution can be carried out on a space grid that remains fixed throughout the calculation, the so-called fixed grid method (Voller,

1987b). In contrast to the variable grid method, domain or coordinate transformation is not required, implying a low computational cost. One of approaches in the fixed grid method, enthalpy method taking account of latent heat evolution, is applied in our calculation. A major advantage of the enthalpy method is that it can calculate the melting with convection by the simple concept of porosity (Brent, 1988). In other words, the combined Enthalpy-Porosity method can accommodate the zero velocity condition which is required as a liquid region turns to solid. Mathematical treatment of this Enthalpy-Porosity method is very simple, and has a wide range of application such as energy storage systems and to casting processes (Yvan et al., 2011; Lamberg et al., 2004; Dawei et al., 2005). For this reason, it was chosen in the current study, and this allows the estimation of the latent heat of melting and the position of the melting front.

A particularly difficult part of the modelling is to compute as a function of time the interface motion and deformation at a flexible free-surface boundary which co-exist with the melting surface. In the case of melting, modelling focuses on the latent heat change with convection flow inside the liquid and melting position of the interface between the liquid and the solid phases, but the key to understanding the free surface motion and the deformation of the melting surface is the surface tension force as well as the tracking free surface. In such problems involving change of phase, diverse approaches exist according to combination of the governing equation and the tracking method, and are divided into roughly two main sectors. These are the Lagrangian or Eulerian approaches for tracking the position of interface based on one or two sets of conservation equations for the phase change. Although two sets of conservation equations with the Lagrangian tracking approaches such as Maker and cell (MAC) methods and the front tracking method (Deen et al., 2009) are quite accurate, nowadays one set conservation equations with the Eulerian approach is more generally used because numerical problems arise when a re-meshing process in Lagrangian tracking approaches is required to model high distortions of interfaces or interface break up. A famous set of conservation equations with Eulerian approach is the VOF (volume of fluid) method, which was pioneered by Hirt and Nichols (Hirt & Nichols, 1981). In this method, the interface is given implicitly by the volume fraction of one of the phases within each cell. A reconstruction of the interface is made, and is propagated implicitly by updating the volume fraction using the transport equation.

Much of the earlier work was performed using the Enthalpy-Porosity method and the VOF method, and have been gradually improved. In order to extend these methods to three phases as in the present study, a combination of melting and free surface tracking is required (Assis et al., 2007; Ganaoui et al., 2002; Jeong et al., 2010; Kamnis & Gu, 2005). For this reason, in the present study numerical model including scalar transport and a source term in the governing equation is considered, and these combined methods are applied to investigate the phenomena during a melting and falls-off process of suspended liquified matter beneath the wire. By exploiting a combination of these two methods melting combined with a three-phase problem is properly considered. Furthermore, for an accurate calculation of the melting and dropping process, temperature dependent surface tension and piecewise polynomial approximation for material properties between solid-liquid phases are additionally applied. In the following, in order to observe the basic process of flame spreading over polymer-coated wire combustion, we are going to model a melting and falls-off process of polymer (i.e., phase change material: PCM) subjected to the local heating without considering any species transport and generation/consumption due to the

chemical reactions. This study is done with commercial software (FLUENT 12.0) based on the finite volume method.

2. Numerical model

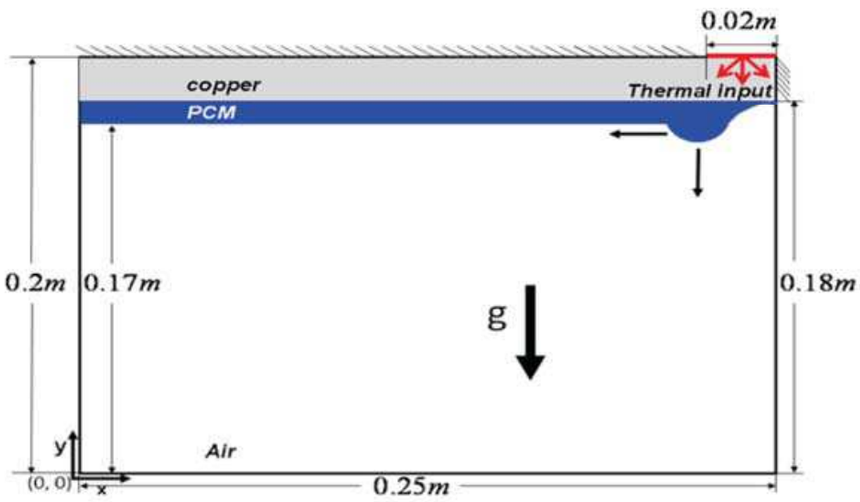

Fig. 2. Schematic description of the numerical model

Fig. 2 is a schematic illustration of the physical configuration. The 2D domain width and height are 0.25 m and 0.2 m respectively, and initially the numerical domain consists of solid (only in the top portion) and gas phases. Solid phase includes copper plate with polymer (phase change material; PCM) whose thickess is 1 mm as shown in Fig.1. Normal gravity, 9.81 m/s^2, is applied in the downward direction. Three materials are used in the calculation, and their properties are described in Table 1. Two phases, liquid & solid, of PCM are included. A localized thermal input is used on the top part of the copper surface. Heat from the localized thermal input is conducted through the copper, and then PCM changes phase from solid to liquid with absorbance of the equivalent latent heat. The free surface of the PCM is then deformed, and liquid PCM moves to the left following the growth of a molten PCM which eventually falls-off via gravity drag.

2.1 Governing equations

Melting of the PCM is governed by the two-dimensional unsteady Navier-Stokes equations in the form of equations for continuity, momentum, and energy.

$$\nabla \cdot (\beta \vec{v}) = 0, \tag{1}$$

$$\beta \frac{\partial \vec{v}}{\partial t} + \nabla \cdot (\beta \vec{v}\vec{v}) = -\frac{\beta}{\rho}\nabla p + \frac{\beta}{\rho}\nabla \cdot [\mu(\nabla \vec{v}) + (\nabla \vec{v})^T] + \beta F_{ST} + \vec{g} + \vec{S}, \tag{2}$$

$$\rho \frac{\partial h}{\partial t} + \nabla \cdot (\rho \vec{v} h) = \nabla \cdot (k\ \nabla T) - S_h. \tag{3}$$

Parameter	Symbol	Value	Units
Air (gas phase)			
Density	ρ_g	1.225	kg/m^3
Thermal conductivity	k_g	0.0242	W/(m K)
Specific heat	$c_{p,g}$	1006.43	J/(kg K)
Viscosity	μ_g	1.789×10^{-5}	kg/(m s)
Copper (solid phase)			
Density	ρ_c	8978	kg/m^3
Thermal conductivity	k_c	387.6	W/(m K)
Specific heat	$c_{p,c}$	381	J/(kg K)
PCM (solid phase)			
Density	ρ_s	980	kg/m^3
Thermal conductivity	k_s	0.24	W/(m K)
Specific heat	$c_{p,s}$	4800	J/(kg K)
Latent heat of melting	L	1.8×10^5	J/kg
Melting temperature	T_m	400	K
PCM (liquid phase)			
Density	ρ_l	900	kg/m^3
Thermal conductivity	k_l	0.15	W/(m K)
Specific heat	$c_{p,l}$	4200	J/(kg K)
Viscosity	μ_l	0.005	kg/(m s)
Solidification temperature	T_s	350	K

Table 1. Physical properties of the phase change material

Here, β is the liquid fraction, $\vec{v}$ is velocity, ρ is density, μ is viscosity, p is pressure, g is gravity, F_{ST} is surface tension force, $\vec{S}$ is the momentum source term, T is temperature, k is conductivity and h is enthalpy. Surface tension is modeled as a smooth variation of capillary pressure across the interface. Following Brackbill et al (Brackbill, 1992), it is represented as a continuum surface force (CSF), and is specified as a volumetric source term in the momentum equation as

$$F_{ST} = \sigma \frac{\rho \kappa_{c,g} \nabla F_g}{0.5(\rho_l + \rho_g)}. \tag{4}$$

Here subscripts g, l and s represent the gas, liquid and solid phase respectively. σ, the surface tension coefficient, is modeled as linear function of temperature, as shown in Fig. 3 . κ_c is the curvature of free surface and is defined in terms of the divergence of the unit normal $\hat{n}$ as

$$\kappa_c = \nabla \bullet \hat{n} \quad \text{with} \quad \hat{n} = \frac{\nabla F}{|\nabla F|}. \tag{5}$$

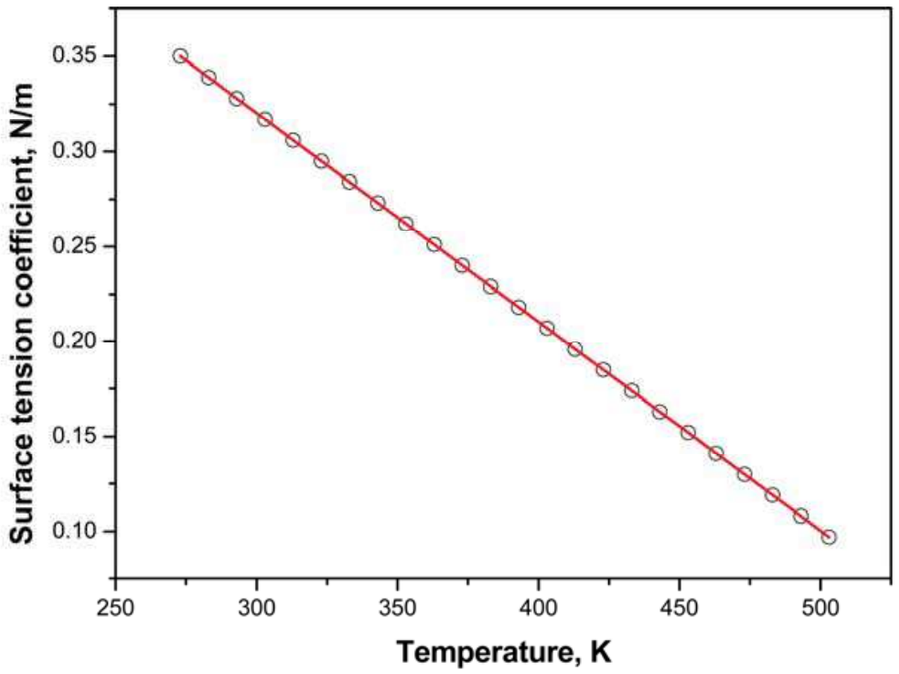

Fig. 3. Surface tension coefficient as a function of temperature

Because surface tension plays an important role in the process of interface reconstruction, a piecewise-linear interpolation scheme developed by Youngs (Youngs, 1982) is used for the interface reconstruction. It assumes that the interface between two fluids has a linear slope within each cell, and uses this linear shape for calculating the advection of fluid through the faces of the computational cell.

In order to model the solid phase, it is necessary to impose a zero velocity on a liquid with the appropriate solid physical parameter. Several methods can be used to achieve this, including velocity switch-off, variable viscosity, and Darcy law approaches (Sanchez-Palencia, 1987). In this work all computational fluid cells were modelled as porous media by adjusting the parameter β. And the Carman-Kozeny equations (Voller, 1987b; Brent, 1988), based on the Darcy law, were used for the source term to describe the flow in the porous medium with the following the momentum equation:

$$\nabla p = -\left[A_{mush} \frac{(1-\beta)^2}{\beta^3} \right] \vec{v}, \tag{6}$$

where A_{mush} is a constant (1.0×10^6) accounting for the mushy region morphology. In order to achieve this behavior, we implemented a source term in the momentum equation for the mushy zone (a region in which the liquid fraction lies between 0 and 1):

$$\vec{S} = -A_{mush} \frac{(1-\beta)^2}{(\beta^3 + \varepsilon)} \vec{v}, \tag{7}$$

where ε is a computational constant (0.001) introduced to prevent division by zero.
In the energy equation, h is the sensible enthalpy, which is

$$h = h_{ref} + \int_{T_{ref}}^{T} c_p dT, \tag{9}$$

where, h_{ref} is the reference enthalpy, T_{ref} is the reference temperature and c_p is specific heat. In the continuity and momentum equation, β determines whether a computational cell is solid or not. β is a function of temperature, and can be described as

$$\beta = \begin{cases} 0 \ if \ T < T_{solidus}, \\ 1 \ if \ T > T_{liquidus}, \\ (T - T_{solidus}) / (T_{liquidus} - T_{solidus}) \ if \ T_{solidus} < T < T_{liquidus}. \end{cases} \tag{10}$$

Furthermore, the energy equation takes into account latent heat as the volume source for the heat transfer condition at the melting front, S_h :

$$S_h = \frac{\partial(\rho \Delta H)}{\partial t} + \nabla \cdot (\rho \vec{v} \Delta H), \tag{11}$$

where ΔH is latent heat, and is defined as $\Delta H = \beta L$, where L is latent heat of PCM material. To represent the free surface of the melting region adjacent to the gas phase, the VOF method is used. In this method, function F is a scalar field, which defines the state of a particular cell in the computational domain:

$$F = \begin{cases} 1 = liquid \ or \ solid, \\ 0 < F < 1 = partial \ gas, \\ 0 = gas, \end{cases} \tag{12}$$

and F also satisfies the conservation equation

$$\frac{DF}{Dt} = \frac{\partial(\beta F)}{\partial t} + \nabla \cdot (\beta \vec{v} F) = 0, \tag{13}$$

and the material properties involved in equations (1) to (3) are written as follows:

$$\rho = \rho_s + \beta(\rho_g - \rho_s) + \beta F(\rho_l - \rho_g), \quad \mu = \beta\mu_g + \beta F(\mu_l - \mu_g)$$
$$k = k_s + \beta(k_g - k_s) + \beta F(k_l - k_g), \quad c_p = c_{p,s} + \beta(c_{p,g} - c_{p,s}) + \beta F(c_{p,l} - c_{p,g}). \tag{14}$$

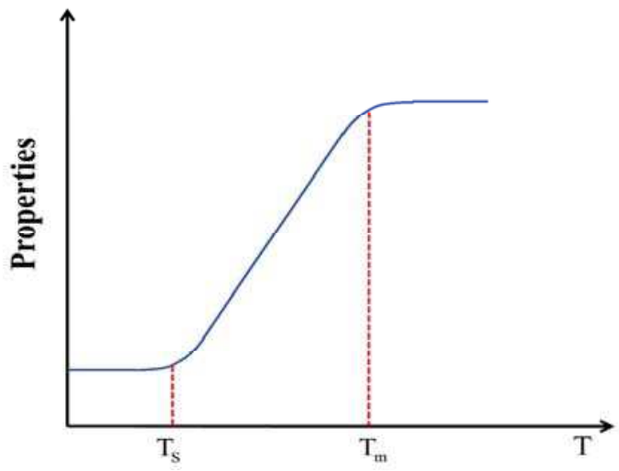

Fig. 4. Temperature dependent smoothed function for modeling properties intermediate between the solid and liquid phases

A smoothed piecewise-polynomial profile, which is a function of temperature, is used due to discontinuities in properties between solid and liquid PCM. This is shown in Fig. 4.

2.2 Initial and boundary conditions

The initial temperature of domain is 300 K, and the localized thermal input temperature is 500 K. The conjugated thermal boundary condition is applied between the copper and the solid PCM, and the heat balance equation between the PCM and air. The boundary conditions are expressed as follows:

at x = 0

$$T = 300\ K;$$

at interface between the PCM and air

$$k_l \frac{\partial T_l}{\partial n} - k_g \frac{\partial T_g}{\partial n} = 0\ ; \tag{15}$$

at interface between the solid and liquid PCM

$$k_s \frac{\partial T_s}{\partial n} - k_l \frac{\partial T_l}{\partial n} = \frac{k}{l}(T_s - T_l)\ ;$$

at other boundaries

$$\frac{\partial T}{\partial x} = 0 \text{ or } \frac{\partial T}{\partial y} = 0.$$

3. Results and discussion

3.1 Model validation

To validate the model, a simple melting problem of gallium in a cavity by the use of Enthalpy-Porosity method was solved and compared with experimental results. Fig. 5 shows the schematic illustration of the physical configuration of gallium melting. Solid gallium occupies the whole domain, T_H = 311 K is heated wall temperature, and T_C = 301.3 K is cold wall temperature. The boundaries of the top and bottom surfaces are isothermal walls. The width W = 8.89 cm and the height H = 6.35 cm. Normal gravity is applied in the downward. Details of the applied material properties and information on the experimental setup are described in Brent's work (Brent, 1988). Once the calculation is started, the solid gallium melts. Fig. 6 shows the shape and location of the solid-liquid interface at several times during the melting process. The black and red lines indicate the experimental (Brent, 1988) and calculated data respectively. Before a time of 2 minutes, the shape of the interface is nearly flat because convection is still weak and melting is driven by conduction. After 2 minutes, the interface becomes wavy due to the circular flow inside the molten region. The position of the melt front near the top surface in the calculation before a time of 12.5 minutes is over-estimated compared to experiment, and after 19 minutes, it is underestimated. However, the overall trend shows good agreement with experiment and we can safely said that our model and code are fairly validated to track the melting boundary satisfactorily. It is well known that a key point in the calculation of melting is the exact interface position between the solid and liquid phases. But in case of a convection-driven melting problem, such exact prediction is difficult due to the complex convection flow inside the liquid. For this reason, numerical studies for convection flow inside molten liquids require more attention (Noureddine, 2003).

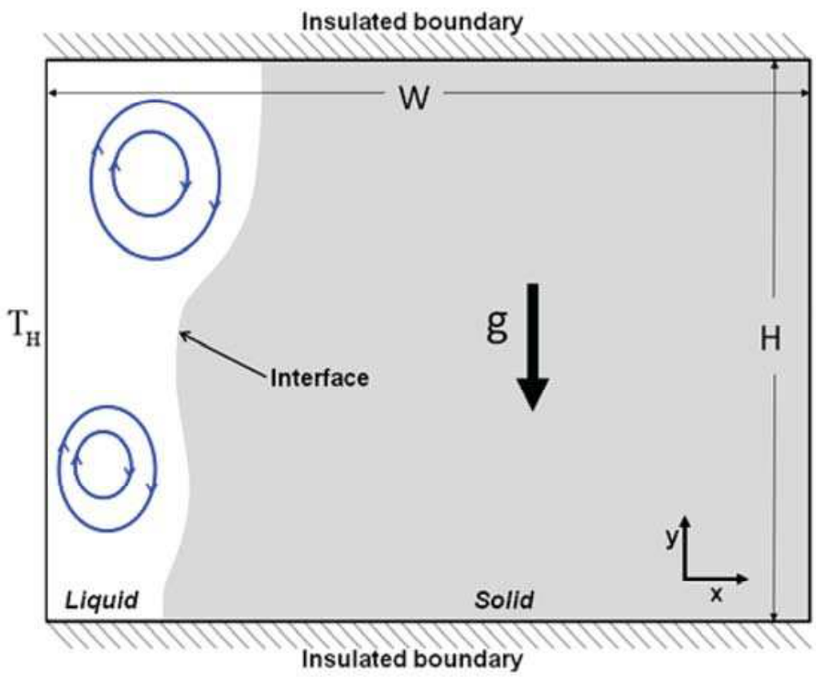

Fig. 5. Schematic of gallium melting

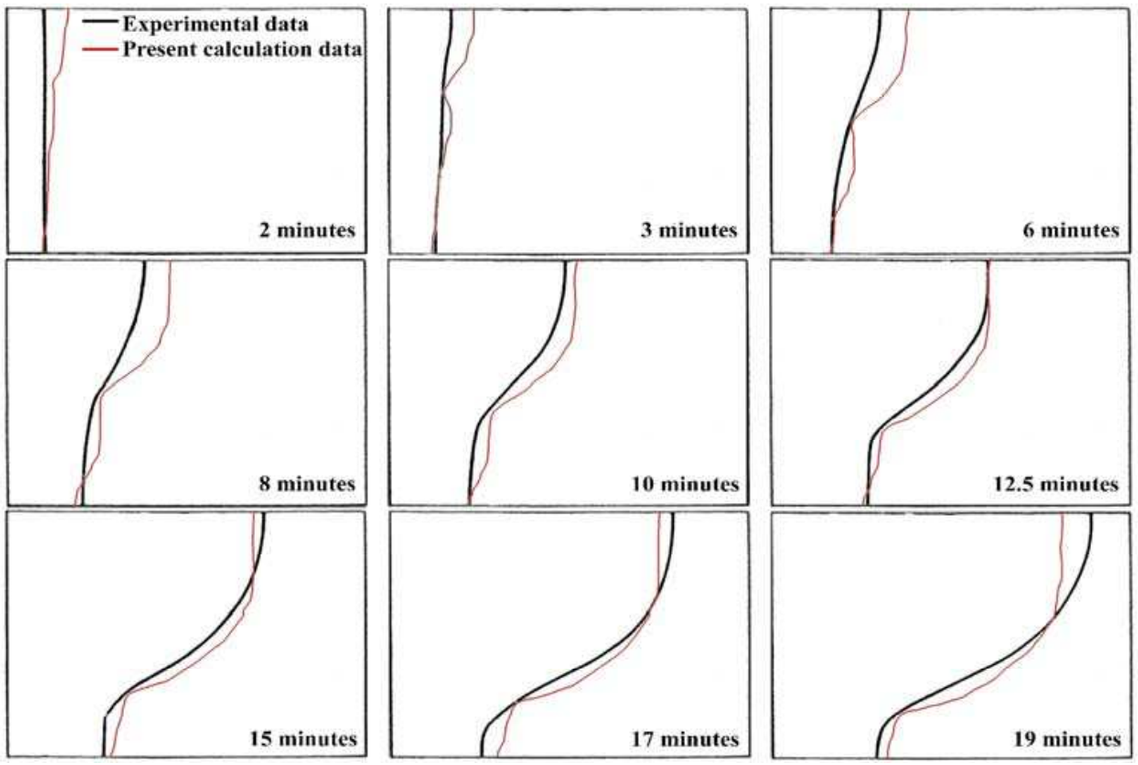

Fig. 6. Comparison of experiment (Brent, 1988) and current numerical model: position of melt front with time

3.2 Expansion to three phase problem

The two dimensional continuity and Navier-Stokes equations are solved with the Enthalpy-Porosity and the VOF methods in order to simulate a melting and falls-off PCM and we can safely said that our model and code are fairly validated to track the melting boundary satisfactorily hereafter. For precise calculation the free interface between liquid PCM and air and linear surface tension, which is function of temperature, are considered. And to reduce the numerical oscillation at the interface discontinuity, a piecewise polynomial profile between the solid and liquid state PCM materials is used.

Energy determines critical point of melting and most physical and transport properties vary with it in melting phenomena. For this reason, at first, the temperature profiles as a function of time at 0, 1, 2, 3.5, 3.9 and 4.2 s are shown in Fig. 7. At 3.9 s, melted PCM separates from the ceiling and falls-off. In this calculation, convection mode heat transfer can be negligible due to no force flow. Heat is transferred by conduction through the copper from the localized thermal input imposed from the right corner at the top surface, and then passed to the PCM and air. At the interface boundary between different materials, a discontinuity in temperature is observed. The temperature profile in all regions shows a decrease over a wide range of y in the air.

Because convection flow inside molten PCM affects the shape of the melt front directly, flow inside molten PCM is shown in Fig. 8 as velocity vectors. During molten PCM growth, the velocity vector is generated inside the molten PCM and then moves to the left. At 3.5 s, a

relatively high surface velocity near the molten ball is observed. When falls-off of molten ball is experienced at 3.9 s, a high velocity driven by gravity is observed.

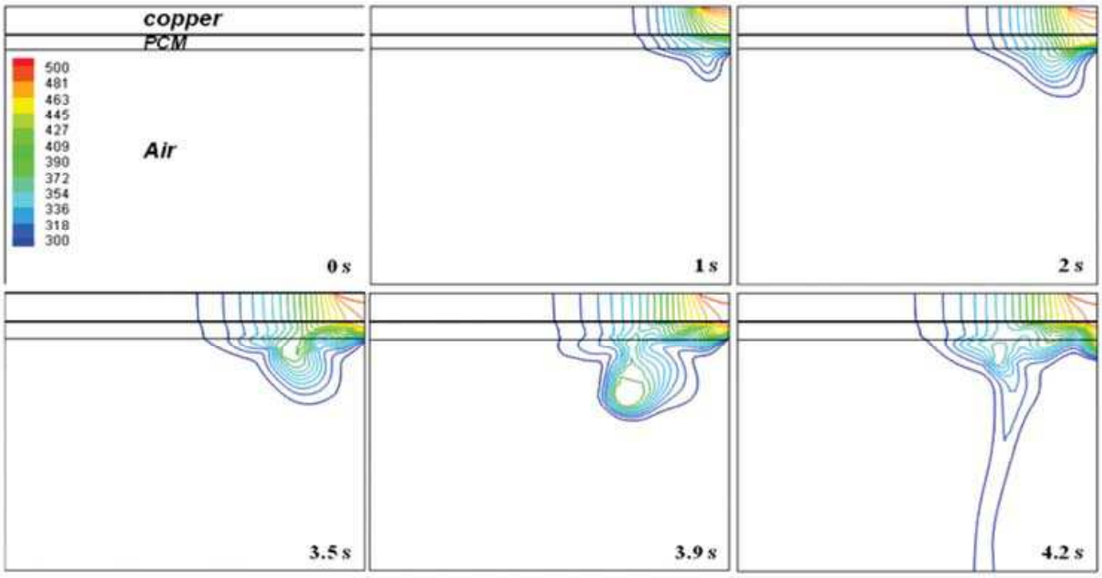

Fig. 7. Temperature distribution in copper, PCM and air as a function of time (localized thermal input is imposed from right side on the top surface of copper)

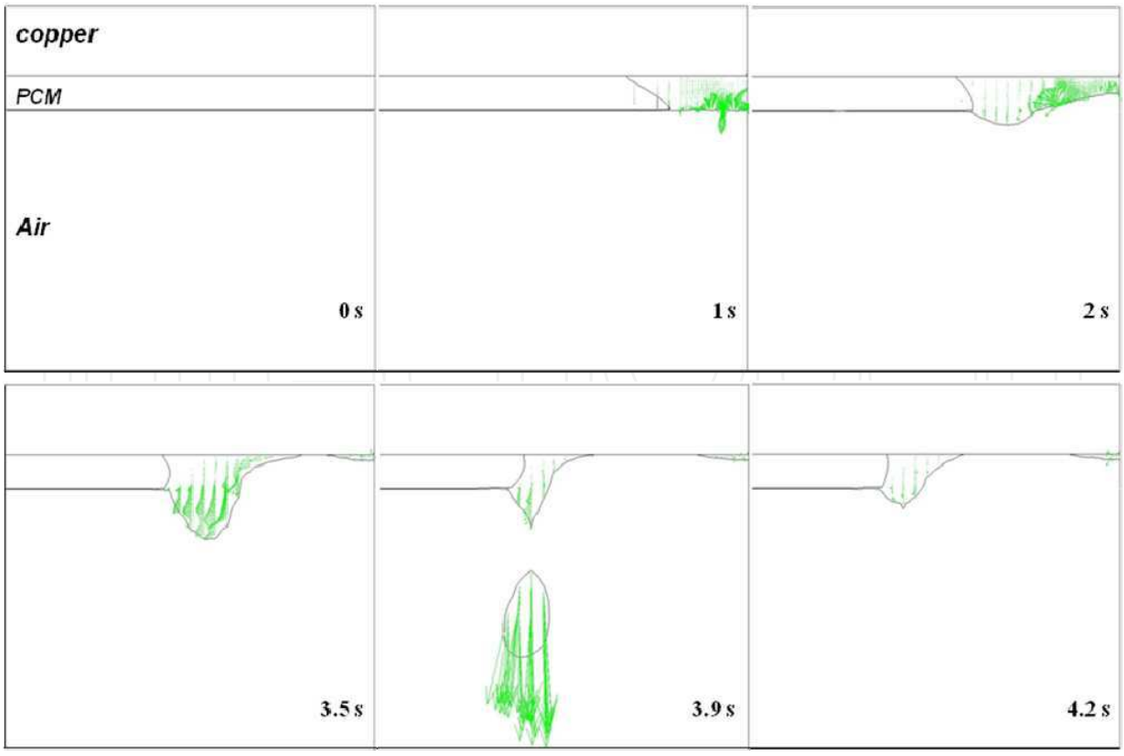

Fig. 8. Velocity vector field and solid-liquid interface at t = 0, 1, 2, 3.5, 3.9 and 4.2 s

Fig. 9 shows the volume fraction, F . In this figure, change of free surface interface between gas and PCM are observed. Free surface interface becomes to strech from 2 s, and then free surface interface moves to left direction. It is important to note that the melted region cannot be distinguished solely by F .

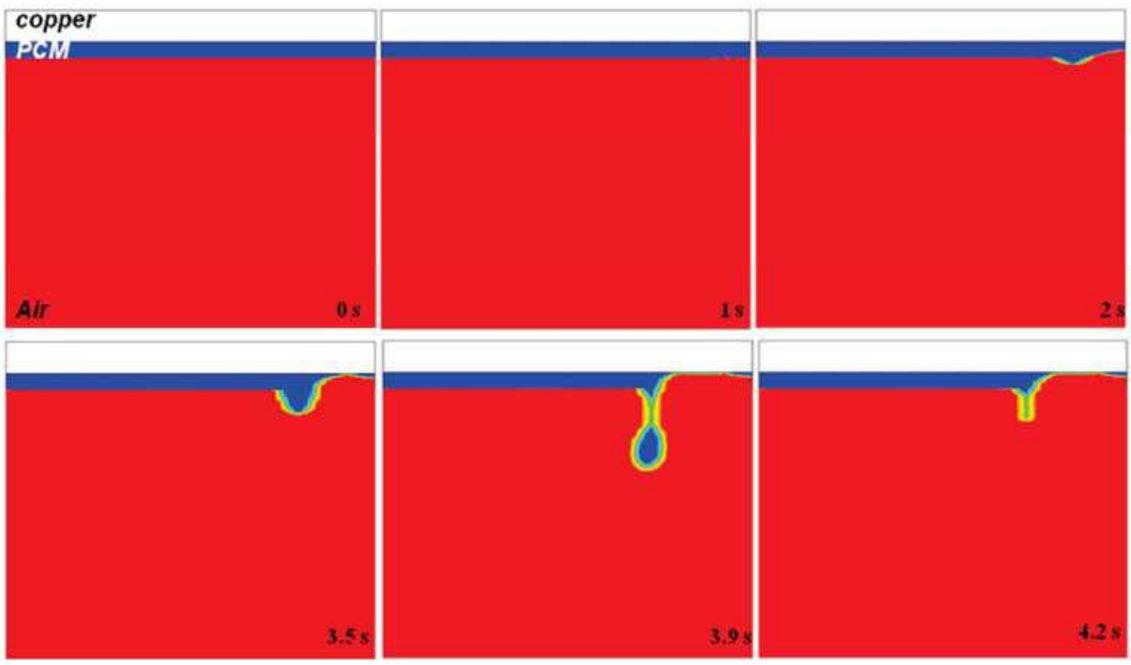

Fig. 9. Time dependence of the volume fraction distribution

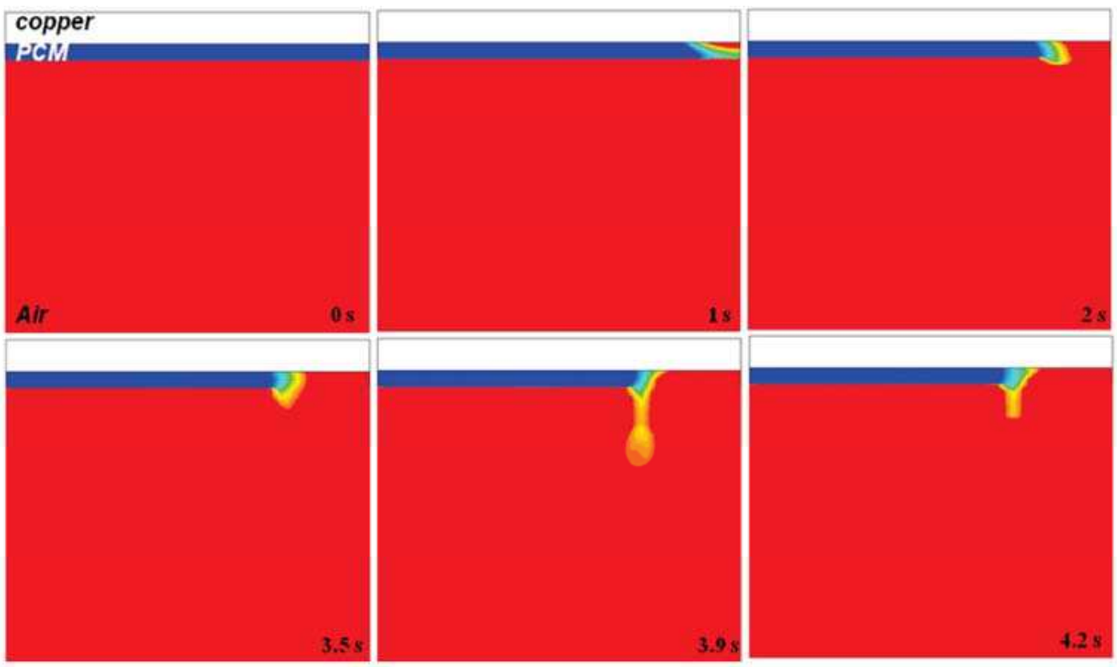

Fig. 10. Time dependence of the liquid fraction distribution

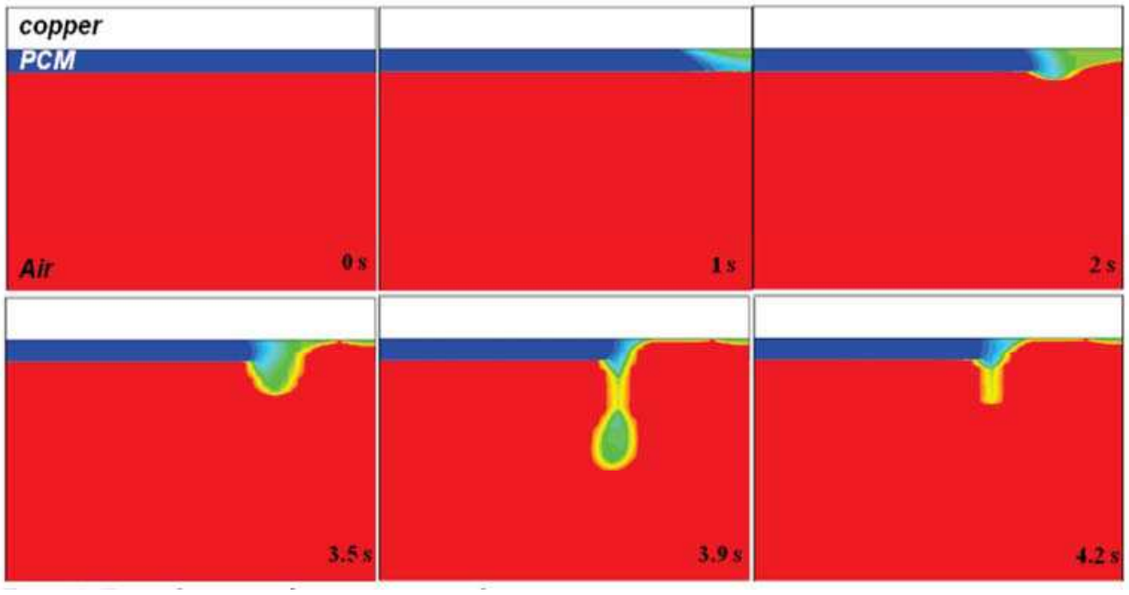

Fig. 11. Distribution of $(\beta + F)/2$ with respect to time

Fig. 10 illustrates the melting processes by use of liquid fraction β. β determines the melt front by both solidus and liquidus temperature. When cell temperature is lower than solidus temperature, $\beta = 0$, mass and momentum equations are turned off, and energy equation is only solved. When cell temperature is higher than liquidus temperature, $\beta = 1$, all equations are solved. If temperature is between solidus and liquidus temperature, $0 < \beta < 1$, cell is treated as partial liquid region, which is represents a mushy region. Here blue is solid region, and red means gas or liquid region. Figure at 1 s shows that melting of PCM begins to happen at the right conner of top surface. After that, melting front advances to left, and then molten ball falls-off at 3.9 s, as stated. But it is hard to distinguish where is liquid and gas region when melt front touch the gas phase. To the end, in order to visualize the three phases together, the simple combined relation, $(\beta + F)/2$, is shown in Fig. 11. When $(\beta + F)/2 = 1$, all computational cells are shown in red, and this represents the gas phase. When $(\beta + F) = 0$, all computational cells are shown in blue, and this represents the solid phase. When $0 < (\beta + F)/2 < 1$, intermediate colors are used to represent the liquid region. Melting in the solid state PCM initially takes place due to absorption of heat from the adjacent copper by localized thermal input. When heat reaches to the free surface between the liquid PCM and air, free surface starts to deform. After that, molten PCM moves to the left and starts to form a molten ball, as shown at 3.5 s. Molten PCM is sustained till 3.9 s, and then the molten ball falls-off eventually. By introducing $(\beta + F)/2$ for identification of edge of each phase, we can see a melting as well as falls-off process clearly.

Fig. 12 represents the melt fraction as a function of time. It is estimated that 24% of the PCM is melted during 4.2 s. Melting of PCM is started at 0.25 s. The melt fraction variation with time exhibits a different gradient after 1.8 s. This behaviour can be categorized by two regimes: regime 1 from the starting point of melting to the point at which the molten ball begins to grow; regime 2 from the point of the initiation of molten ball growth and the point at which molten ball starts to drop. These two regimes can be explained by different

conduction modes. In regime 1, the conduction from copper governs the heat transfer to the solid PCM, and this directly affects the melt fraction. However, liquefied PCM on the right hand side moves to the left, and then it generates the molten ball. Therefore, when the melt front becomes isolated from the localized thermal input, it is more affected by the molten ball than by the copper. So in regime 2, heat transfer by conduction from the molten ball dominates the melt fraction rather than that from copper. This can be more easily understood by observing the shape of solid PCM adjacent to the melt front and the melt fraction after the molten ball falls-off (as it is shown by the inset in Fig.12). Within regime 1, the top part of the solid PCM is more melted than the bottom part because the conduction mode of heat transfer from the copper mainly affects the PCM. However in the case of regime 2, the bottom part of the solid PCM is more melted than the top part because the molten ball governs the heat transfer to the solid PCM rather than from the copper. It is also seen that after the falls-off the molten ball, the melt speed is dramatically reduced. This fact could support above-mentioned thermal status, such that the heat from the molten ball is mainly governed by melting phenomena in the PCM before the falling-off is experienced.

$(\beta + F)/2$ are shown with various surface tension coefficients, [σ] in Figs. 13, 14 and 15. Falling-off of molten phase is only happen in Fig. 13 (surface tension coefficient; [σ] = 0.15), and is repeated. But when relatively high surface tension is forced, free surface of molten PCM is sustained along the copper, and melted region is broadening out, which is shown in Figs. 14 and 15. Especially, in case of surface tension [σ] = 0.35, surface becomes wavy, and molten ball is not generated till 4.2 s. The surface tension force is a tensile force tangential to the interface separating pair of fluids, and it tries to keep the fluid molecules at the free surface. Therefore, molten PCM can be sustained with growth of forced surface tension.

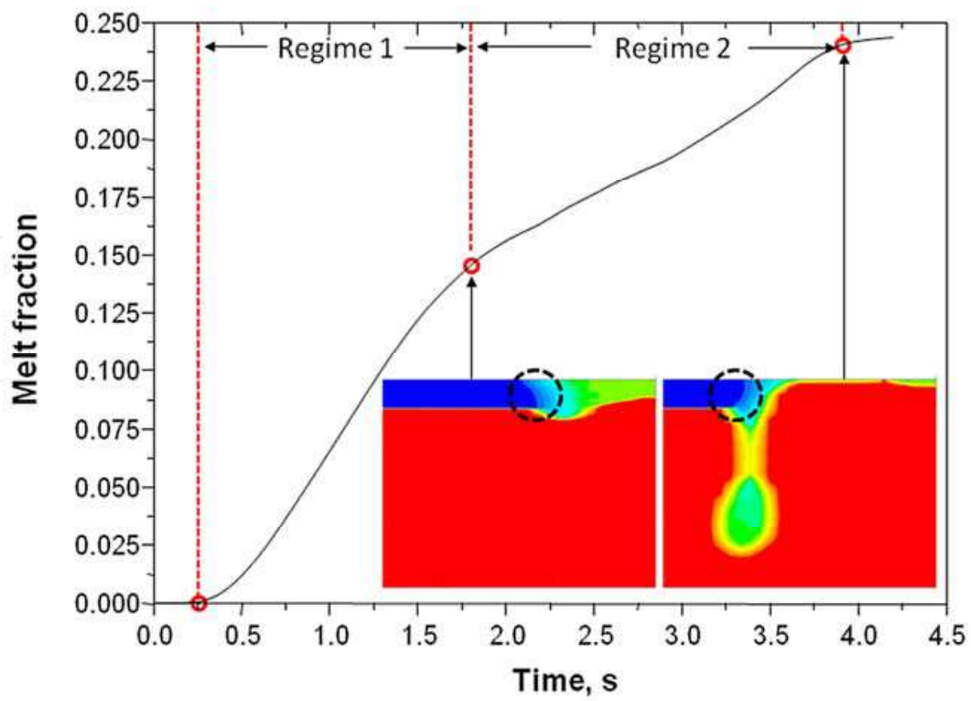

Fig. 12. Melt fraction with time, showing two regimes

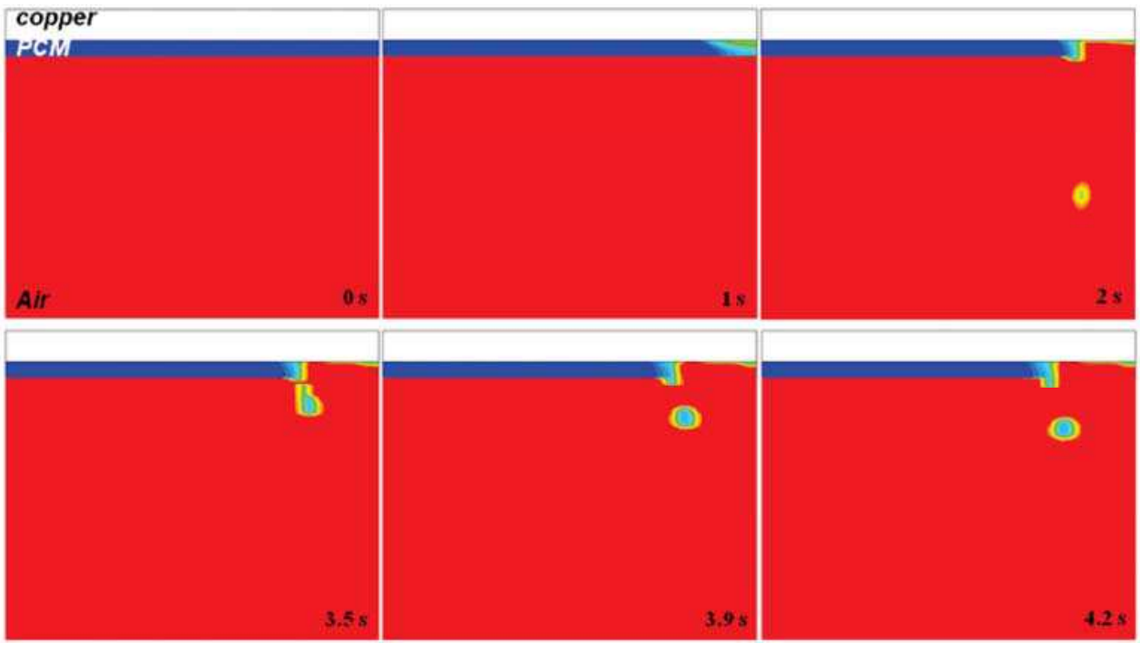

Fig. 13. Distribution of $(\beta + F)/2$ with respect to time (surface tension coefficient, [σ] = 0.15)

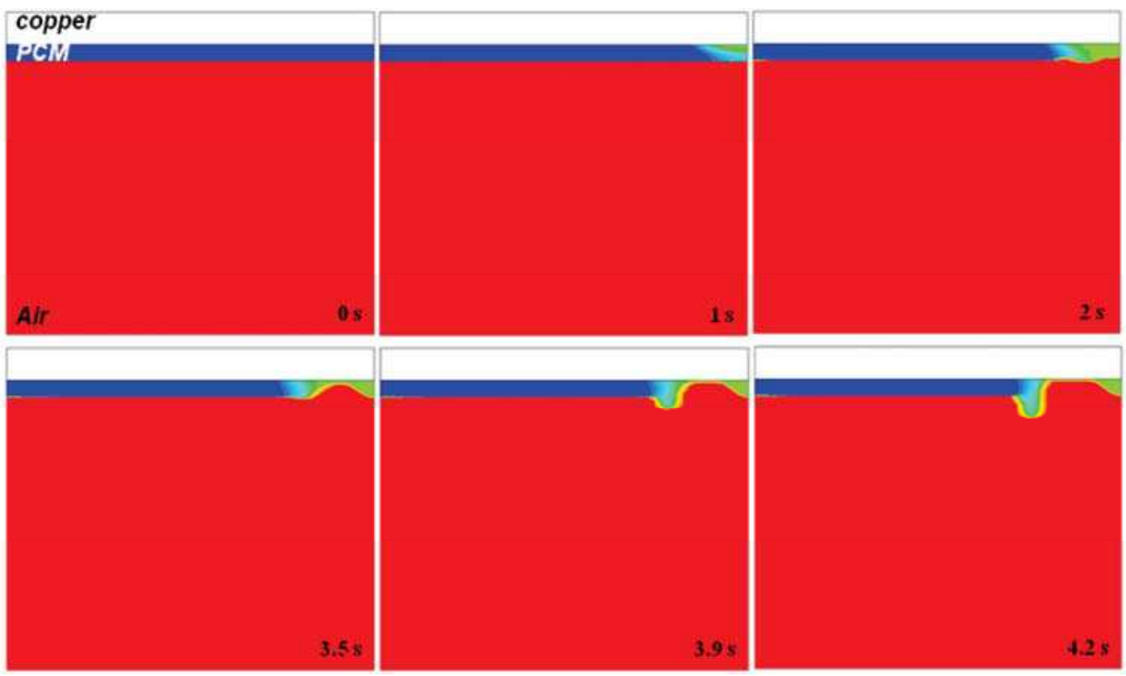

Fig. 14. Distribution of $(\beta + F)/2$ with respect to time ([σ] = 0.25)

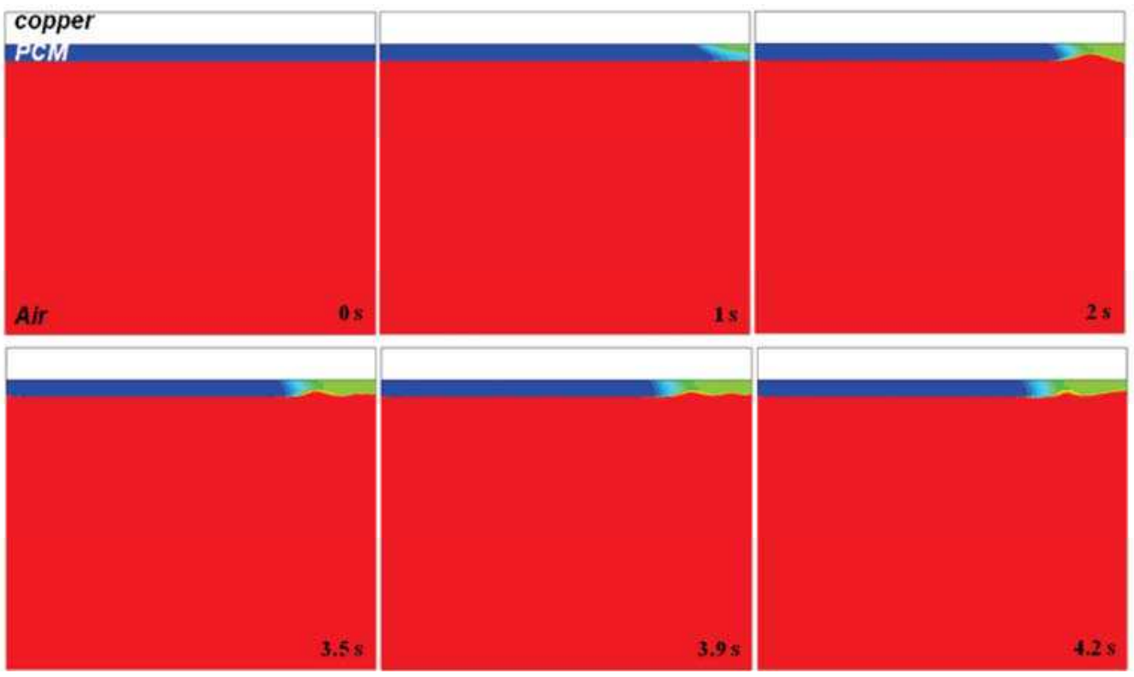

Fig. 15. Distribution of $(\beta + F)/2$ with respect to time ([σ] = 0.35)

4. Conclusion

The model proposed in this study has been successfully applied in the elucidation of the melting process involving three phases and the falling-off phenomena of sustained solid matter. The Enthalpy-Porosity and VOF methods generate scalar transport and involve source term in the governing equations. Additional treatment for surface tension and material properties at the interface between solid and liquid PCM are applied. Validation of the current model by existing experiment shows reasonable agreement from the mathematical as well as from the physical points of view. Discontinuity at the phase interface is inherently included in the governing equation at each time step. However this may generate errors during the progression of time. Therefore we precisely included heat transfer, motion of molten ball and melting rate in the model to minimize such errors. Furthermore we suggested that there are two different dominant modes during the melting and falls-off process: one is the copper conduction driven mode and the other is the molten PCM driven mode. Finally, possible effect induced by surface tension on heat transfer in PCM was elucidated. Although the model requires further development and validation of the model with the inclusion of much more complex phenomena such as species transport and combustion processes, and this study has brought one of major insights of teat transfer which possibly occurs during the wire combustion.

5. Acknowledgment

The authors gratefully acknowledge the financial support for this research provided by JSPS (Grants-in-aid for Young Scientists: #21681022; PI: YN) and the Japan Nuclear Energy Safety

Organization (JNES). The first author (YK) also would like to express his sincere appreciation to the Ministry of Education, Culture, Sports, Science and Technology, Japan for providing him the MEXT Scholarship for conducting this research.

6. References

Assis, E.; Katsman, L.; Ziskind, G. & Letan, R. (2007). Numerical and Experimental Study of Melting in a Spherical Shell, *International Journal of Heat and Mass Transfer*, Vol. 50, pp. 1790-1804.

Bakhman, N. N.; Aldabaev, L. I.; Kondrikov, B. N. & Filippov, V. A. (1981a). Burning of Polymeric Coatings on Copper Wires and Glass Threads : I. Flame Propagation Velocity, *Combust. Flame*, Vol. 41, pp. 17-34.

Bakhman, N. N.; Aldabaev, L. I.; Kondrikov, B. N. & Filippov, V. A. (1981b). Burning of Polymeric Coatings on Copper Wires and Glass Threads : II. Critical Conditions of Burning, *Combust. Flame*, Vol. 41, pp. 35-43.

Brackbill, J. U.; Kothe, D. B. & Zemach, C. (1992). A Continuum Method for Modeling Surface Tension, *Journal of Computational Physics*, Vol. 100, No. 2, pp. 335-354.

Brent, A. D.; Voller, V. R. & Reid, K. J. (1988). The Enthalpy-Porosity Technique for Modeling Convection-Diffusion Phase Change : Application to the Melting of a Pure Metal, *Numerical Heat Transfer*, Vol. 13, pp. 297-318.

Dawei, S.; Suresh, V. G.; Sanjeev, S. & Neelam, N. (2005). Numerical and Experimental Investigation of the Melt Casting of Explosives, *Propellants, Explosives, Pyrotechnics*, Vol. 30, No. 5, pp. 369-380.

Deen, N. G.; Annaland, M. V. S. & Kuipers, J. A. M. (2009). Direct Numerical Simulation of Complex Multi-fluid Flows Using a Combined Front Tracking and Immersed Boundary Method, *Chemical Engineering Science*, Vol. 64, pp. 2186-2201.

Di Blasi, C.; Crescitelli, S. & Russo, G. (1991). Model of Oscillatory Phenomena of Flame Spread along the Surface of Liquid Fuels, *Comp. Meth. App. Mech. Eng*, Vol. 90, pp. 643-657.

FLUENT 12. 0 User's Guide, Available from http://www.ansys.com

Ganaoui, M. E.; Lamazouade, A. ; Bontoux, P. & Morvan, D. (2002). Computational Solution for Fluid Flow under Solid/liquid Phase Change Conditions, *Computers & Fluids*, Vol. 31, pp. 539-556.

Gong, Z. X. & Mujumdar, A. S. (1997). Flow and Heat Transfer in Convection-dominated Melting in a Rectangular Cavity Heated from Below, *International Journal of Heat and Mass Transfer*, Vol. 41, No. 17, pp. 2573-2580.

Gong, Z. X. ; Devahastin, S. & Mujumdar, A. S. (1999). Enhanced Heat Trasnfer in Free Convection-dominated Melting in a Rectangular Cavity with an Isothermal Vertical Wall, *Applied Thermal Engineering*, Vol. 19, No. 12, pp. 1237-1251.

Hirt, C. W. & Nichols, B. D. (1981). Volume of Fluid (VOF) Method for the Dynamics of Free Boundaries, *Journal of computational Physics*, Vol. 39, pp. 201-225.

Jeong, H.; Lee, Y.; Ji, M. ; Lee, G. & Chung, H. (2010). The Optimum Solidification and Crucible Rotation in Silicon Czochralski Crystal Growth, *Journal of Mechanical Science and Technology*, Vol. 24, pp. 407-414.

Kamnis, S. & Gu, S. (2005). Numerical Modelling of Droplet Impingement, *Journal of Physics D: Applied Physics*, Vol. 38, pp. 3664-3673.

Lamberg, P.; Lehtiniemi, R. & Henell, A. (2004). Numerical and Experimental Investigation of Melting and Freezing Processes in Phase Change Material Storage, *International Journal of Thermal Sciences*, Vol. 43, No. 3, pp. 277-287.

McCabe, W. L.; Smith, J. C. & Harriot, P. (2005). *Unit Operations of Chemical Engineering* (7th ed.), McGraw-Hill, New York, pp. 163-165.

Nakamura, Y.; Yoshimura, N.; Ito, H.; Azumaya, K. & Fujita, O. (2008a). Flame Spread over Electric Wire in Sub-atmospheric Pressure, *Proceedings of the Combustion Institute*, Vol. 32, No. 2, pp. 2559-2562.

Nakamura, Y.; Yoshimura, N.; Matsumura, T.; Ito, H. & Fujita, O. (2008b). Opposed-wind Effect on Flame Spread of Electric Wire in Sub-atmospheric Pressure, *Thermal Sci. Tech*, Vol. 3, No. 3, pp. 430-441.

Nakamura, Y.; Azumaya, K.; Ito, H. & Fujita, O. (2009). Time-dependent Flame Spread Behavior of Electric Wire in Sub-atmospheric Pressure, *9th Proc. Asia-Pacific Conference on Combustion*, pp. 101, Taipei, Taiwan May, 2009.

Neumann, F. (1863). Experiments on the Thermal Conductivity of Solids, *Phill. Mag*. 25, 63.

Noureddine H. (2003). Resolving the Controversy over Tin and Gallium Melting in a Rectangular Cavity Heated from the Side, *Numerical Heat Transfer, Part B*, Vol. 44, pp. 253-276.

Ross, H. D. (1994). Ignition of and Flame Spread over Laboratory-scale Pools of Pure Liquid Fuels, *Prog. Energy Combust. Sci*, Vol. 20, pp. 17-63.

Sanchez-Palencia, E. (1987). Homogenization Techniques for Composite Media, *Lecture Notes in Physics,* Springer-Verlag, New York.

Umemura, A.; Uchida, M.; Hirata, T. & Sato, J. (2002). Physical Model Analysis of Flame Spreading along an Electric Wire in Microgravity, *Combust. Inst*, Vol. 29, pp. 2535-2543.

Voller, V. R. (1986). An Implicit Enthalpy Solution for Phase Change Problems : With Application to a Binary Alloy Solidifiaction, *Applied Mathematical Modelling,* Vol.11, No.2 pp. 110-116.

Voller, V. R. (1987a). An Enthalpy Method for Convection/diffusion Phase Change, *International Journal for Numeirical Methods in Engineering,* Vol. 24, pp. 271-284.

Voller, V. R. (1987b). A Fixed Grid Numerical Modelling Methodology for Convection-diffusion Mushy Region Phase-change Problems, *International Journal of Heat and Mass Transfer*, Vol. 30, No. 8, pp. 1709-1719.

Yang, H. & He, Y. (2010). Solving Heat Transfer Problems with Phase Change via Smoothed Effective Heat Capacity and Element-free Galerkin Methods, *International Communications in Heat and Mass Transfer*, Vol. 37, No. 4, pp. 385-392.

Youngs, D. L. (1982). Time Dependent Multimatierial Flow with Large Fluid Distortion, *Numerical Methods for Fluid Dynamics,* pp. 273-285.

Yvan, D.; Daniel, R. R.; Nizar, B. S.; Stéphane L. & Laurent, Z. (2011). A Review on Phase-change Materials : Mathematical Modeling and Simulations, *Renewable and Sustainable Energy Reviews*, Vol. 15, pp. 112-330.

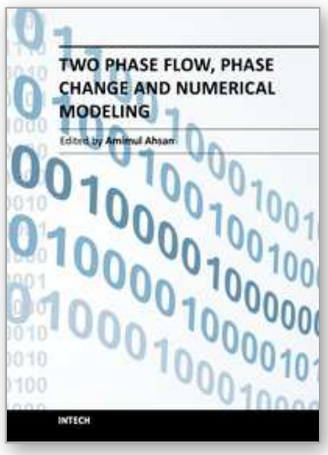

Two Phase Flow, Phase Change and Numerical Modeling
Edited by Dr. Amimul Ahsan

ISBN 978-953-307-584-6
Hard cover, 584 pages
Publisher InTech
Published online 26, September, 2011
Published in print edition September, 2011

The heat transfer and analysis on laser beam, evaporator coils, shell-and-tube condenser, two phase flow, nanofluids, complex fluids, and on phase change are significant issues in a design of wide range of industrial processes and devices. This book includes 25 advanced and revised contributions, and it covers mainly (1) numerical modeling of heat transfer, (2) two phase flow, (3) nanofluids, and (4) phase change. The first section introduces numerical modeling of heat transfer on particles in binary gas-solid fluidization bed, solidification phenomena, thermal approaches to laser damage, and temperature and velocity distribution. The second section covers density wave instability phenomena, gas and spray-water quenching, spray cooling, wettability effect, liquid film thickness, and thermosyphon loop. The third section includes nanofluids for heat transfer, nanofluids in minichannels, potential and engineering strategies on nanofluids, and heat transfer at nanoscale. The forth section presents time-dependent melting and deformation processes of phase change material (PCM), thermal energy storage tanks using PCM, phase change in deep CO2 injector, and thermal storage device of solar hot water system. The advanced idea and information described here will be fruitful for the readers to find a sustainable solution in an industrialized society.

How to reference
In order to correctly reference this scholarly work, feel free to copy and paste the following:

Yangkyun Kim, Akter Hossain, Sungcho Kim and Yuji Nakamura (2011). A Numerical Study on Time-Dependent Melting and Deformation Processes of Phase Change Material (PCM) Induced by Localized Thermal Input, Two Phase Flow, Phase Change and Numerical Modeling, Dr. Amimul Ahsan (Ed.), ISBN: 978-953-307-584-6, InTech, Available from: http://www.intechopen.com/books/two-phase-flow-phase-change-and-numerical-modeling/a-numerical-study-on-time-dependent-melting-and-deformation-processes-of-phase-change-material-pcm-i

INTECH
open science | open minds

InTech Europe
University Campus STeP Ri
Slavka Krautzeka 83/A
51000 Rijeka, Croatia
Phone: +385 (51) 770 447
Fax: +385 (51) 686 166

InTech China
Unit 405, Office Block, Hotel Equatorial Shanghai
No.65, Yan An Road (West), Shanghai, 200040, China
中国上海市延安西路65号上海国际贵都大饭店办公楼405单元
Phone: +86-21-62489820
Fax: +86-21-62489821

IntechOpen

IntechOpen